Interim Report   IR-13-055

Adaptive phenotypic diversification along a temperature-depth gradient

Jan Ohlberger
Åke Brännström (brnstrom@iiasa.ac.at)
Ulf Dieckmann (dieckmann@iiasa.ac.at)

Approved by

Pavel Kabat
Director General and Chief Executive Officer

June 2015

1 *Manuscript type*: Article

2

3 **Adaptive phenotypic diversification along a temperature-depth gradient**

4 Jan Ohlberger[1,2,3,*], Åke Brännström[3,4,#], Ulf Dieckmann[3,+]

5

6 [1] Department of Biology and Ecology of Fishes, Leibniz-Institute of Freshwater Ecology and Inland Fisheries,

7 D-12587 Berlin, Germany

8 [2] Centre for Ecological and Evolutionary Synthesis, Department of Biology, University of Oslo, N-0316 Oslo,

9 Norway

10 [3] Evolution and Ecology Program, International Institute for Applied Systems Analysis, A-2361 Laxenburg,

11 Austria

12 [4] Department of Mathematics and Mathematical Statistics, Umeå University, SE-90187 Umeå, Sweden

13 [*] jan.ohlberger@bio.uio.no (corresponding author)

14 [#] ake.brannstrom@math.umu.se

15 [+] dieckmann@iiasa.ac.at

16

17 *Keywords*: adaptive dynamics, ecological gradient, evolutionary diversification, sympatric

18 speciation, temperature adaptation

19 *Online appendix A*: Model variables, functions, and parameters

20 *Online appendix B*: Model functions and their estimation from empirical data

21 *Online appendix C*: Sensitivity analysis

22   **ABSTRACT**

23   Theoretical models suggest that sympatric speciation along environmental gradients might be

24   common in nature. Here we present the first data-based model of evolutionary diversification

25   along a continuous environmental gradient. Based on genetic analyses, it has been suggested

26   that a pair of coregonid fishes (*Coregonus* spp.) in a postglacial German lake originated by

27   sympatric speciation. Within this lake, the two species segregate vertically and show

28   metabolic adaptations to, as well as behavioral preferences for, correspondingly different

29   temperatures. We test the plausibility of the hypothesis that this diversifying process has been

30   driven by adaptations to different thermal microhabitats along the lake's temperature-depth

31   gradient. Using an adaptive dynamics model that is calibrated with empirical data and that

32   allows the gradual evolution of a quantitative trait describing optimal foraging temperature,

33   we show that under the specific environmental conditions in the lake, evolutionary branching

34   of a hypothetical ancestral population into two distinct phenotypes may have occurred. We

35   also show that the resultant evolutionary diversification yields two stably coexisting

36   populations with trait values and depth distributions that are in agreement with those currently

37   observed in the lake. We conclude that divergent thermal adaptations along the temperature-

38   depth gradient might have brought about the two species observed today.

INTRODUCTION

Understanding the emergence of biological diversity by adaptive diversification based on natural selection is a major interest in evolutionary biology. The notion of adaptive speciation suggests that macro-evolutionary phenomena of diversification are ultimately the outcome of micro-evolutionary processes driven by natural selection in general (Orr and Smith 1998; Coyne and Orr 2004), and by frequency-dependent disruptive selection in particular (Dieckmann et al. 2004). Following this notion, the formation of phenotypic and ecological diversity is likely to imply disruptive natural selection arising from competitive interactions. Competitive interactions between individuals and populations within the same geographical area – independently of whether they result from exploitation competition, interference competition, or apparent competition – are thus of major importance for understanding biological diversification. Empirical studies have confirmed that intraspecific competition can be frequency-dependent (e.g., Swanson et al. 2003; Schluter 2003), making disruptive selection on corresponding traits of natural populations more likely than previously thought (Bolnick and Lau 2008). Frequency dependence occurs whenever selection pressures depend on the phenotypic composition of a population, which is a direct and often inevitable consequence of the way a population shapes the environment it in turn experiences.

The geographical conditions underlying diversifying processes have long been a focus of debate (e.g., Mayr 1963; Via 2001). However, the mechanisms of ecologically based sympatric, parapatric, and allopatric speciation that can drive divergence appear to be similar, with disruptive or divergent natural selection on ecologically important traits serving as the driving force of diversification, and with the evolution of reproductive isolation occurring as a consequence of divergent selection on those traits (Schluter 2000). There is now mounting empirical evidence for the operation of ecological speciation in nature (Schluter 2009; Nosil 2012). The process of ecologically based adaptive speciation does not only necessitate the

64   emergence of reproductive isolation during diversification, but also requires the ability of the

65   incipient species to coexist persistently (Coyne and Orr 2004). Hence, the same ecological

66   conditions and mechanisms that facilitate disruptive natural selection can cause adaptive

67   speciation through gradually divergent evolution, promote reproductive isolation between the

68   incipient species, and enable the coexistence of closely related species in sympatry.

69   Highlighting one common mode of ecological speciation, empirical work suggests that

70   competition-driven divergent resource or habitat use plays an important role in causing

71   ecological diversification (Svanbäck and Bolnick 2007) and in promoting sympatric

72   speciation (e.g., Gislason et al. 1999; Knudsen et al. 2006) within natural populations. With

73   this study, we aim to identify ecological conditions that potentially drive adaptive

74   diversifications in sympatry, as well as the underlying phenotypic traits that are subject to

75   disruptive natural selection.

76   The theory of adaptive dynamics (Metz et al. 1992, 1996; Dieckmann and Law 1996;

77   Geritz et al. 1998) has facilitated the construction of theoretical models investigating

78   ecologically based processes of evolutionary diversification (Doebeli and Dieckmann 2005).

79   Addressing this objective is aided by the assumption, often made in the theory of adaptive

80   dynamics, that there is a sufficient separation of the timescales on which ecological change

81   and evolutionary changes unfold. The resultant framework allows evaluating the potential for

82   evolutionary diversification in complex adaptive systems with an emphasis on the ecological

83   conditions promoting the corresponding selection pressures on specific adaptive traits of

84   natural populations. Frequency-dependent selection on a slowly evolving quantitative trait of

85   an asexually reproducing population leads to directional evolution along the local selection

86   gradient until an evolutionarily singular strategy is reached. This singular strategy can either

87   be a fitness maximum, and hence be locally evolutionarily stable for a single morph, or it can

88   be a fitness minimum, and hence be an 'evolutionary branching point', which potentially

89   leads to the splitting and subsequent divergence of two genetically distinct morphs. Adaptive

90   dynamics models have repeatedly shown that many natural ecological settings are expected to

91   imply evolution to such fitness minima, at which evolutionary branching may then occur

92   based on frequency-dependent disruptive selection (as reviewed, e.g., in Dieckmann et al.

93   2004; see also Ito and Dieckmann 2007). In accordance with the majority of empirical

94   examples of adaptive diversification, most of the existing adaptive-speciation models assume

95   ecological specialization through resource partitioning as the key driver of diversification.

96   One conclusion from advanced adaptive-speciation models is that sympatric speciation

97   is theoretically plausible and may thus be a common process in nature (e.g., Dieckmann and

98   Doebeli 1999). However, theoretical speciation models are not easily evaluated in terms of

99   biological plausibility and may lack ecological realism or accuracy in their assumptions about

100 the properties of natural systems. For instance, the parameter regions in which evolutionary

101 branching may occur in such models is usually only indirectly comparable among different

102 models, and quantitative comparisons to natural systems are often difficult to make without

103 referring to one particular natural system. Data-based models of adaptive diversification,

104 utilizing empirically motivated and quantitative ecological assumptions, are therefore needed

105 to evaluate the importance of these processes in nature.

106   The main purpose of this study is to develop such an empirically motivated and data-

107 based model for adaptive diversification in a specific natural system that has already been

108 well investigated (*Coregonus* spp. in Lake Stechlin, Germany). The model aims to describe

109 the diversification of a single ancestral population into two stably coexisting populations by

110 physiological adaptation to different thermal microhabitats along a temperature-depth

111 gradient in a temperate freshwater lake. Our model does not consider the genetic architecture

112 of the quantitative trait involved in this process and is not meant to examine the evolution of

113 reproductive isolation. We rather examine whether the ecological conditions in our study lake

114 allow for the evolution of an ancestral population toward a fitness minimum and the

115 subsequent evolutionary branching.

116 **MATERIALS AND METHODS**

117 **Model system**

118 Temperate freshwater fish occupying postglacial lakes are among the best model systems for

119 studying adaptive diversification. Several taxa in these systems exhibit an ecological diversity

120 consistent with processes of adaptive speciation (Schluter 2000), including the coregonids

121 (reviewed in Hudson et al. 2007). In the deep postglacial Lake Stechlin in Germany

122 (maximum depth 69m), a pair of closely related coregonids coexists: common vendace

123 (*Coregonus albula* L.) and endemic dwarf-sized Fontane cisco (*Coregonus fontanae* Schulz

124 and Freyhof). The two species are easily distinguished by differential spawning times and

125 show distinct morphological characteristics (Schulz and Freyhof 2003; Helland et al. 2009).

126 Their sympatric evolution has been suggested based on mtDNA and microsatellite analyses

127 (Schulz et al. 2006). Recent AFLP analyses could neither confirm nor reject this hypothesis

128 (Mehner et al. 2010a). The species differ in their average population depths within the pelagic

129 zone, with *C. fontanae* being found deeper in the water column than *C. albula* throughout the

130 year. This difference in depth distribution is associated with a difference in mean experienced

131 water temperature (Helland et al. 2007; Mehner et al. 2010b).

132   Despite the depth segregation, diet compositions of the species are rather similar, with

133 a clear dominance of planktonic food (Helland et al. 2008). Hence, mechanisms reducing

134 competition and thus potentially driving divergence between the species are not significantly

135 related to diet. Instead, an important factor promoting ecological divergence between the

136 species is a difference in temperature-dependent metabolic costs of swimming (Ohlberger et

137 al. 2008a). This directly influences the competitive abilities of the two populations via their

138   efficiency of foraging at a specific temperature, and thus depth. Furthermore, the temperature

139   preferences of the two species correspond to the temperatures at which their net costs of

140   swimming are minimized (Ohlberger et al. 2008c), which underscores the role of temperature

141   as the predominant environmental factor shaping the divergence between the two coregonids.

142   This setting offers a unique opportunity for investigating whether the observed conditions

143   allow for ecological and evolutionary diversification of pelagic fish populations along the

144   temperature-depth gradient of the lake.

145   **Model description**

146   We modeled asexual fish populations competing for the same zooplankton resource with a

147   depth-dependent carrying capacity along a temperature-depth gradient $T(x)$, where T

148   denotes temperature and x denotes depth. The fish populations can adapt to different ambient

149   temperature conditions, i.e., to different locations along the depth axis, through adaptations in

150   a one-dimensional quantitative trait, which specifies the temperature-dependent metabolic

151   optimum, or optimum foraging temperature. For a fish morph i, with $i = 1,...,n$, this trait

152   value is denoted by T_i. For describing the evolutionary dynamics of the trait values, we

153   assume asexual reproduction, a low mutation probability μ, and a small standard deviation

154   σ of mutational steps, so that evolution follows the canonical equation of adaptive dynamics

155   (Dieckmann and Law 1996) in conjunction with fitness-based conditions for evolutionary

156   branching (Geritz et al. 1998), as specified in detail below. For a didactical introduction to,

157   and further details on, the adaptive dynamics approach, see, e.g., Diekmann (2004).

158   The fish population dynamics are deterministic and structured with regard to depth x,

159   with $0 < x < x_{max}$. Exploitation competition for zooplankton, considered as the predominant

160   cause of competition among fish in our model, is logistic and occurs at each depth. The

161   foraging efficiency $r(T, T_i)$ of a fish morph i, with $i = 1,...,n$, is assumed to drop with

162   temperature T on both sides around the morph-specific optimum foraging temperature T_i.

163   The maximum zooplankton density is described by the depth-dependent carrying-capacity

164   density $K(x)$, which declines monotonically with depth. The gain in biomass density $B_i(x)$

165   of morph i at depth x, which includes fecundity, is proportional to the potential consumption

166   rate and the equilibrium zooplankton density. Biomass loss, which includes mortality, arises

167   from maintenance costs $m(T)$, which monotonically decrease with temperature. Therefore,

168   the per capita growth rates $f_i(x)$, in terms of biomass, are given by the difference between

169   per capita resource intake rates and per capita maintenance costs. We denote by f_i the

170   average growth of morph i across all depths x. We further assume the rapid redistribution of

171   individuals along the temperature-depth gradient following foraging dynamics, which in our

172   model can be chosen from a continuum between random foraging and optimal foraging by

173   varying a parameter α. Individuals keep adjusting their depth according to their potential

174   consumption rate, their potential predation risk, and resource availability.

175   In addition to the morph indices $i = 1,...,n$ for the n resident morphs, we use $i = 0$ for

176   a rare mutant. The growth rate f_0 of such a rare mutant equals its invasion fitness (Metz et al.

177   1992), with its first derivative (often called selection gradient or fitness gradient) denoted by

178   g_i, and its second derivative denoted by h_i. These derivatives of invasion fitness are taken

179   with respect to the mutant trait value T_0 and are evaluated at the trait value of the resident

180   with trait value T_i. Online appendix A provides an overview of all variables, functions, and

181   parameters used in this study.

182   **Model dynamics**

183   The population dynamics are described by the change in total biomass of fish morph i over

184   time,

185 $$\frac{d}{dt} B_i = f_i B_i,$$

186 where B_i is the total biomass and f_i is the average growth rate of morph i. The total biomass

187 is given by the integral of biomass density from zero to maximum depth,

188 $$B_i = \int_0^{x_{max}} B_i(x)\,dx,$$

189 where $B_i(x)$ is the biomass density of morph i at depth x. The average growth rate of morph

190 i is thus given by

191 $$f_i = \frac{1}{B_i} \int_0^{x_{max}} f_i(x) B_i(x)\,dx,$$

192 with

193 $$f_i(x) = \lambda C(x, T_i) P_{eq}(x) - m(T(x)),$$

194 where λ is the conversion factor from zooplankton mass to fish mass (i.e., the energy-

195 assimilation efficiency of the fish), $f_i(x)$ is the morph's per capita growth rate at depth x,

196 $C(x, T_i)$ is the potential consumption rate of morph i with trait T_i at depth x, $P_{eq}(x)$ is the

197 equilibrium zooplankton density at depth x, and $m(T)$ measures the temperature-dependent

198 maintenance costs. We thus assume that feeding under natural conditions can be

199 approximated by a linear relationship with resource density. We also assume fast resource

200 dynamics, so that the zooplankton density is always near its equilibrium (Online appendix B).

201   For the adaptive foraging dynamics, we assume that an individual fish with trait T_i

202 adjusts its depth according to its potential consumption rate $C(x, T_i)$, the equilibrium

203 zooplankton density $P_{eq}(x)$, and a foraging probability $F(x)$ that accounts for the depth-

204 dependent risk of predation by piscivorous predators,

205 $$B_i(x) = B_i \frac{[C(x, T_i) P_{eq}(x) F(x)]^{\alpha}}{\int_0^{x_{max}} [C(x', T_i) P_{eq}(x') F(x')]^{\alpha}\,dx'},$$

9

206   where α is the degree of foraging optimality (with $\alpha = 0$ representing random foraging and

207     $\alpha \to \infty$ representing optimal foraging).

208   The expected evolutionary dynamics of the trait value T_i describing the metabolic

209   temperature optimum of morph i, is given by the canonical equation of adaptive dynamics

210   (Dieckmann and Law 1996),

211          $$\frac{d}{dt} T_i \propto B_i g_i,$$

212   where B_i is the equilibrium population size and g_i is the first derivative of a mutant's invasion

213   fitness, i.e., the selection gradient. More details on the evolutionary analysis are provided

214   under the corresponding heading below.

215   **Parameter estimation**

216   Data sources for all parameter estimates are provided in Online appendix A. Fig. 1 and Online

217   appendix B provide details on the estimation of functions describing the temperature-depth

218   gradient, observed zooplankton density, potential consumption rate, foraging efficiency,

219   capture success, maintenance costs, and foraging probability. These functions and parameters

220   were estimated based on observational data from Lake Stechlin in conjunction with various

221   laboratory measurements on the two coregonids. The foraging optimality α was estimated

222   based on the distribution patterns of the two coregonids in Lake Stechlin. This parameter

223   measures the degree to which individuals forage at their temperature optimum. In order to

224   estimate the degree of foraging optimality in the natural system, we ran our model without

225   evolutionary dynamics for the empirically determined temperature optima as fixed trait values

226   and compare the resulting average depths with the measured year-round average depths of the

227   Lake Stechlin coregonids (Helland et al. 2007). A figure provided in the online appendix

228   (Fig. B1) shows, as a function of α, the sum of absolute values of the deviations of the two

229   modeled population depths from the two observed average population depths in the natural

230   system. A foraging optimality α of about 6 was found to offer the best approximation for the

231   foraging behavior of these fish. We thus use this α-value in our further analyses.

232   **Evolutionary analysis**

233   We use a pairwise invasibility analysis to investigate the evolutionary dynamics in our system

234   under the specific ecological conditions encountered in Lake Stechlin. Pairwise invasibility

235   analysis assumes that any mutant introduced to the system first occurs at very low numbers

236   and that the resident population has come sufficiently close to its demographic equilibrium at

237   the time a mutant is introduced (Van Tienderen and De Jong 1986; Metz et al. 1992).

238   To evaluate the potential for directional evolution on the adaptive trait of an

239   established resident population, we need to calculate the invasion fitness of a mutant with a

240   trait value that slightly differs from that of the resident (Metz et al. 1992). This invasion

241   fitness is given by the sum of the mutant's growth rates across all depths, evaluated at the

242   demographic equilibrium of the resident population (Online appendix B). In case of positive

243   invasion fitness, the mutant generically replaces the resident (Geritz et al. 2002) and the

244   resident population's trait value shifts accordingly. This directional selection on the trait of a

245   monomorphic resident population persists as long as the selection gradient

246        $$g_i = \frac{\partial}{\partial T_0} f_0 \Big|_{T_0 = T_i}$$

247   remains positive or negative. The point at which directional evolution comes to a halt is

248   referred to as an 'evolutionarily singular strategy' (Metz et al. 1996).

249   Once evolution has reached such a singular strategy, selection becomes either

250   stabilizing or disruptive, depending on the local shape of the fitness landscape described by

251   f_0 as a function of T_0. If the singular strategy is located at a local fitness maximum, no more

252   invasion of any nearby mutant morph is possible, so that the singular strategy is evolutionarily

253   stable. If the singular strategy is instead located at a local fitness minimum, it is evolutionary

11

254 unstable. This means that all nearby mutant morphs can invade the system and establish a

255 second resident population, so the system becomes dimorphic. A strategy at which selection

256 becomes disruptive and to which directional evolution can nevertheless converge is known as

257 an 'evolutionary branching point' (Metz et al. 1992, 1996; Geritz et al. 1998). Evolutionary

258 branching can occur if the second derivative of the invasion fitness,

259 $$h_i = \left. \frac{\partial^2}{\partial T_0^2} f_0 \right|_{T_0 = T_i},$$

260 is positive. An evolutionary branching point implies that a mutant can invade and stably

261 coexist with the resident population. In other words, an evolutionary branching point can give

262 rise to a protected dimorphism, in which each of the two morphs can invade the other.

263   The direction of dimorphic evolution after evolutionary branching is determined

264 analogously to the monomorphic case. This is achieved by testing a system with two

265 established residents for invasibility by a mutant. If a mutant close to one of the residents has

266 positive invasion fitness, it successfully invades the system and replaces that resident. Such

267 dimorphic directional evolution then proceeds until a strategy pair is reached at which the two

268 selection gradients vanish. At this point, further evolutionary branching may occur, if at least

269 one of the populations is situated at a fitness minimum. Otherwise, evolution comes to a halt.

270 **Sexual reproduction**

271 We incorporate sexual reproduction into the model following standard procedures

272 (Roughgarden 1979; Bulmer 1980). In the asexual model, the phenotype is normally

273 faithfully inherited from parent to offspring, except for mutations occurring with small

274 probability. In contrast, in the sexual model, offspring phenotypes are always subject to

275 variation resulting from genetic segregation and recombination. Also, mating is assortative, so

276 individuals pair up for reproduction based on their similarity in trait value.

277   Specifically, an individual j with trait value T_j mates with another individual k

278   with trait value T_k according to a Gaussian probability distribution around its trait value with

279   standard deviation σ_a,

280        $$K_{\mathrm{a}}(T_j, T_k) = \exp(-\tfrac{1}{2}(T_j - T_k)^2 / \sigma_{\mathrm{a}}^2) / (\sqrt{2\pi}\,\sigma_{\mathrm{a}}).$$

281   Thus, σ_a measures the width of the mating kernel K_{a}, and therefore determines the degree of

282   assortment, with large σ_a corresponding to random mating and smaller σ_a corresponding to

283   increasingly assortative mating. The probability that phenotype j reproduces with phenotype

284   k further depends on the frequency F_k of that phenotype in the population. Assuming a

285   discretized trait space with a finite number n of possible phenotypes, $T_i = 1, \ldots, n$, the

286   frequency F_k is given by

287        $$F_k = B_k / \sum_{i=1}^{n} B_i.$$

288   To account for the effects of genetic segregation and recombination, the offspring trait

289   value T_i is drawn from the following probability density,

290        $$K_{\mathrm{sr}}(T_i, T_j, T_k) = \exp(-\tfrac{1}{2}(T_{jk} - T_i)^2 / \sigma_{\mathrm{sr}}^2) / (\sqrt{2\pi}\,\sigma_{\mathrm{sr}}),$$

291   i.e., from a Gaussian distribution around the mid-parental trait value $T_{jk} = (T_j + T_k) / 2$, with

292   standard deviation σ_{sr}. Thus, σ_{sr} measures the width of the segregation-recombination kernel

293   (Roughgarden 1979), which describes the distribution of offspring traits for given parents.

294   This approach assumes that the variation introduced by the segregation and recombination of

295   genes is constant over time (Roughgarden 1979).

296   The probability density to be born with trait value T_i for a given maternal trait value

297   T_j depends on the frequency distribution of phenotypes in the population, the degree of

298   assortment, and the variation with which the offspring trait value is inherited from the parents,

299
$$w(T_i, T_j) = Z_{ij}^{-1} \sum_{k=1}^{n} F_k K_a(T_j, T_k) K_{sr}(T_i, T_j, T_k),$$

300   where the normalization constant $Z_{ij} = \sum_{i,k=0}^{n} F_k K_a(T_j, T_k) K_{sr}(T_i, T_j, T_k)$ is chosen so that

301    $\sum_{i=0}^{n} w(T_i, T_j) = 1$. Hence, the probability to be born with trait value T_i from all possible

302   matings is given by

303
$$w(T_i) = \sum_{j=1}^{n} F_j w(T_i, T_j).$$

304   To determine whether the evolved trait distribution in the sexual model is unimodal

305   (representing a single species) or bimodal (representing two specialist species), we directly

306   compare the biomass densities of the phenotypic class adapted to $T_i = 8.1°C$ (corresponding

307   to the evolutionarily singular strategy in the asexual model) to the biomass densities of the

308   phenotypic classes adapted to $T_i = 5°C$ and $T_i = 10°C$ (corresponding to the two specialists at

309   the evolutionary endpoint of the asexual model). When the intermediate class is less frequent

310   than both the warm-adapted and the cold-adapted classes, we consider the outcome of the

311   sexual model to represent two distinct morphs. As for the asexual model, we use numerical

312   analyses to investigate the sexual model.

313   **RESULTS**

314   To investigate the evolutionary dynamics of our asexual model and to answer the question

315   whether evolutionary branching may occur under the specific ecological conditions specified

316   by the data-based parameter estimates and empirically motivated structural model

317   assumptions, we apply the methods of evolutionary analysis described above. We visualize

318   our results using a 'pairwise invasibility plot' (PIP) and a 'trait-evolution plot' (TEP; Geritz et

319   al. 1998). Furthermore, to investigate the dynamics of the sexual model, we evaluate how the

320   evolutionary outcome is determined by the widths of the mating kernel (degree of assortment)

321   and the segregation-recombination kernel (offspring distribution).

322   Fig. 2 shows the PIP for all trait-value combinations of a resident and a mutant morph

323   with temperature optima between 4°C and 12°C for a foraging optimality α of 6. A

324   monomorphic population starting with any trait value is subject to directional selection and

325   therefore evolves until the singular strategy is reached at about 8.1°C. At this point, the

326   population experiences a fitness minimum and selection becomes disruptive, so that

327   evolutionary branching can occur.

328   Fig. 3 provides a TEP to visualize the subset of trait combinations for which the two

329   morphs are able to coexist in a protected dimorphism (grey area). It also depicts the direction

330   of selection gradients (arrows), the evolutionary isoclines along which one of the selection

331   gradients vanishes (continuous and dotted lines), and the expected course of dimorphic

332   directional evolution after evolutionary branching (dashed lines). Within the area of

333   coexistence, the two morphs evolve to a point (large filled circles) at which the two isoclines

334   intersect. The resultant trait combinations are 5.0°C and 10.0°C. At these trait combinations,

335   both selection gradients vanish and directional selection for the two morphs thus ceases. Since

336   both isoclines are at a local fitness maximum at their intersection, the resulting dimorphism is

337   locally evolutionarily stable. Hence, no secondary evolutionary branching can take place in

338   the system, and the two morphs are recognized as the model-predicted evolutionary outcome.

339   Fig. 4 compares the model-predicted trait values and biomass distributions with the

340   empirically observed trait values and biomass distributions. Fig. 4A shows time series of the

341   evolving monomorphic and dimorphic optimum foraging temperatures, and compares the

342   latter with the observed temperature preferences of the two coregonids in Lake Stechlin. The

343   initial trait value of the monomorphic population does not alter the evolutionary outcome,

344   since the evolutionary branching point is globally convergence stable (i.e., a monomorphic

345   population evolves towards this point irrespective of its initial value). The temperature optima

346   at the endpoint of dimorphic evolution (5.0°C and 10.0°C) are in good agreement with the

347   measured temperature preferences of the two coregonids (4.2°C and 9.0°C) (Ohlberger et al.

348   2008c). Fig. 4B shows the depth distributions of the two morphs after dimorphic evolution

349   has come to a halt and compares their average depths with the year-round average depths

350   observed for the coregonids in Lake Stechlin. This comparison shows that the model-

351   predicted average depths of the populations at the endpoint of dimorphic evolution match

352   very well those observed in the field (Helland et al. 2007).

353   Fig. 5 displays the evolutionary outcome for the sexual model in dependence on the

354   functions describing assortative mating and segregation/recombination. The diagram shows

355   that speciation becomes more likely as the standard deviations of these two kernels decrease.

356   For low degrees of assortment (high σ_a), and for a wide offspring trait distribution around the

357   mid-parental trait value (high σ_{sr}), the population remains monomorphic, centered around a

358   trait value of about 8°C. The threshold for the width of the assortative-mating kernel above

359   which diversification cannot occur is ca. 0.9, which means that a focal individual choosing

360   between two potential mates is 65% as likely to choose a mate whose trait value differs by

361   1°C than to choose a mate with its own trait value. The threshold for the width of the

362   segregation-recombination kernel above which diversification cannot occur is ca. 0.6, which

363   means that the offspring trait value has a probability of ca. 90% to differ by less than 1°C

364   from the mid-parental trait value. Our results show that the two thresholds for the assortative-

365   mating kernel and the segregation-recombination kernel are fairly independent of each other.

366   Finally, Fig. 6 shows a trait-evolution plot for the sexual model for a given degree of

367   assortment ($\sigma_a = 0.2$) and a given variance of the offspring trait distribution ($\sigma_{sr} = 0.2$). This

368   setting yields a dimorphic outcome, with the highest biomass densities at trait values around

369   5°C and 10°C, which is in accordance with the values we have identified above for the

370   asexual model and with the values that have been reported for the empirically observed

371   thermal-preference traits of the two species (Ohlberger et al. 2008c).

372   A main target parameter for a sensitivity analysis of our model is the foraging

373   optimality α, since the evolutionary dynamics are much affected by this parameter. An α-

374   value of less than about 1 results in a monomorphic evolutionarily stable strategy at an

375   intermediate temperature optimum, whereas values larger than about 10 may lead to

376   secondary evolutionary branching, and thus to the evolutionary establishment of higher

377   degrees of polymorphism. It is therefore reassuring to confirm that even considerable

378   variations in α (over the range of 1 to 10, compared with the value of $\alpha = 6$ estimated from

379   the empirical distribution patterns of the two coregonids in the lake; Fig. B1) do not have a

380   qualitative effect on the evolutionary outcome in our model. We note, however, that, as

381   higher values of α approximate the foraging behavior of the fish reasonably well (Fig. 1B),

382   the ecological conditions in the lake might favor multiple evolutionary branching. In that

383   case, other factors such as the degree of assortment or the distribution of offspring trait values

384   could have prevented a second diversification event among the studied coregonids. All other

385   model parameters are based on empirical data from Lake Stechlin and the species pair, are

386   direct system characteristics, or have been taken from other literature on coregonids (Online

387   appendix A). In order to account for uncertainty in the empirically derived parameters and to

388   check the robustness of our results to changes in these parameters, we performed a univariate

389   sensitivity analysis by increasing or decreasing each parameter value by 10% and evaluating

390   the resulting trait values at the evolutionary endpoint of the asexual model (Table C1). All

391   considered parameter perturbations allow for evolutionary branching and result in trait values

392   for the two morphs that are similar to those predicted by the non-perturbed model – which

393   means that they are also similar to the experimentally determined trait values of the two

394   coregonids. The trait value of the cold-adapted phenotype (4.6-5.5°C) was most strongly

395   affected by changes in the minimum temperature at lake bottom (T_{min}), i.e., by the lower

396   thermal limit of the habitat available to the fish. The trait value of the warm-adapted

397   phenotype (9.1-10.8°C) was most strongly affected by changes in the maximum temperature

398   at which the fish forage (T_{max}), i.e., by the upper thermal limit of their habitat (Online

399   appendix C).

400   **DISCUSSION**

401   It is widely believed that the same ecological conditions that produce disruptive selection and

402   cause adaptive speciation drive the ecological differentiation that enables the coexistence of

403   closely related species in sympatry (Schluter 2000; Coyne and Orr 2004). Previous empirical

404   studies on the species pair in Lake Stechlin had revealed that the two coexisting coregonids

405   have diverged with respect to their vertical distribution in the lake (Helland et al. 2007,

406   2009), the temperature-dependence of their metabolism (Ohlberger et al. 2008a), and their

407   associated thermal preferences (Ohlberger et al. 2008c). The concordance in the ecological,

408   physiological, and behavioral differentiation of the species with respect to temperature

409   suggests thermal specialization as the main driver of their eco-evolutionary divergence. This

410   divergence may have originated from two preexisting species through character displacement,

411   or from a single ancestral species through sympatric speciation, with the latter option being

412   supported by genetic analyses (Schulz et al. 2006; Mehner et al. 2010a).

413   We have shown by analyses of the evolutionary dynamics of the model introduced in

414   this study, that under the specific empirical conditions observed in Lake Stechlin (*i*)

415   evolutionary branching of a single ancestral population into two morphs with distinct thermal

18

416 specialization should have been favored by the ecological conditions, that (*ii*) the two model-

417 predicted populations can stably coexist, and (*iii*) that they have temperature optima and

418 depth distributions that closely correspond to those in the field. The model thereby supports

419 the hypothesis that the temperature-depth gradient in this system has mediated the thermal

420 specialization of the two species, thereby allowing them to occupy different thermal niches

421 along the vertical lake axis. This result clearly contrasts with the commonly observed

422 divergence of many other sympatric fish pairs, especially in newly colonized postglacial

423 lakes. The common situation in these lakes is the occurrence of limnetic-benthic species pairs

424 that have diverged into distinct ecotypes or species by exploiting either benthic food in

425 profundal or littoral habitats, or planktonic food in pelagic habitats, giving rise to an

426 ecological pattern known as trophic polymorphism (Schluter and McPhail 1993; Lu and

427 Bernatchez 1999; Knudsen et al. 2006). Our results are in line with recent findings suggesting

428 that divergent thermal adaptation of sibling taxa caused by differential selection between

429 thermal environments may underlie reproductive isolation or allow for stable coexistence in

430 several animal and plant systems (Keller and Seehausen 2012).

431 To our knowledge, we present the first data-based model of adaptive diversification

432 along a continuous environmental gradient. Based on our model analyses, we conclude that

433 the ecological conditions in Lake Stechlin are prone to evolutionary branching, and that

434 sympatric speciation of coregonids in this lake is thus an ecologically plausible scenario.

435 Since the hypothesized speciation process occurs along an environmental gradient, i.e., along

436 a spatial dimension in our model, it possesses elements of parapatric speciation. However,

437 since isolation by distance is not expected to play any significant role over the short spatial

438 ranges that characterize the vertical differentiation of the two species, the particular speciation

439 process modeled here presumably is very close to the sympatric end along the sympatric-

440 allopatric continuum of parapatric speciation. Other authors who have attempted to describe

441 the evolutionary dynamics of a particular system based on empirical data have used models in

442 which selection (acting on several traits) is density-dependent and the environment is

443 represented by a number of novel and discrete ecological niches (e.g., Gavrilets and Vose

444 2007; Gavrilets et al. 2007). The main advantage of an empirically calibrated mathematical

445 model of adaptive speciation is its ability to help identify the crucial environmental factors in

446 processes of evolutionary diversification. Previously, the theory of adaptive dynamics has

447 been successfully applied to developing various strategic models of sympatric and parapatric

448 speciation, although its usefulness for approaching evolutionary problems has occasionally

449 been challenged (e.g., Gavrilets 2005; Waxman and Gavrilets 2005). Our work here, although

450 limited by the underlying simplifying assumptions and by a focus on one specific natural

451 system, shows that adaptive dynamics theory also offers useful tools for identifying, through

452 interfacing with the relevant empirical data, key ecological factors involved in processes of

453 evolutionary diversification under natural conditions.

454   The endpoint of evolutionary dynamics in our model describes a dimorphic fish

455 population consisting of one morph with a lower temperature optimum that occupies deeper

456 water layers relative to another morph with a higher temperature optimum that occupies

457 shallower water layers (with optimum foraging temperatures of 5.0°C and 10.0°C,

458 respectively). This model outcome matches the experimentally determined species-specific

459 thermal preferences and corresponding temperatures of lowest swimming costs (4.2°C and

460 9.0°C; Ohlberger et al. 2008a,c), and is in good accordance with the experienced water

461 temperatures of the coregonids in Lake Stechlin (4.0-6.0°C and 6.5-9.0°C; Mehner et al.

462 2010b). These comparisons show that the two populations that evolve in our model well

463 represent the natural populations in terms of their distributions and trait values. Interestingly,

464 Lake Stechlin and the nearby Lake Breiter Luzin are the only two lakes in Germany in which

465 sympatric pairs of coregonids occur. Both are located at the southern border of the *C. albula*

466   distribution range (Kottelat and Freyhof 2007) and are the deepest in that region (Mehner et

467   al. 2005), thus featuring the broadest temperature ranges and steepest gradients among lakes

468   worldwide in which *C. albula* occurs (Kottelat and Freyhof 2007). Besides temperature, light

469   intensity decreases continuously with lake depth. This might have facilitated a differentiation

470   in light-dependent feeding efficiencies along the depth gradient. However, there is good

471   evidence that the two species do not differ in their foraging efficiency at light intensities

472   experienced in the lake (Ohlberger et al. 2008b). Other factors that might have facilitated the

473   evolutionary divergence of an ancestral population include a species-poor environment and a

474   high level of intraspecific competition at the time of colonization, conditions that are often

475   found in newly colonized postglacial lakes, and are believed to promote ecologically based

476   adaptive diversification in fishes (Vamosi 2003; Bolnick 2004).

477   Environmental temperature gradients are common phenomena in nature, with a major

478   effect on biogeographical patterns of species distributions. For instance, the large-scale

479   biogeography and the small-scale distribution of fishes are broadly shaped by temperature

480   patterns (Somero 2002, 2005; Pörtner et al. 2007, 2010). Furthermore, it has been reported

481   that niche segregation of fishes can be facilitated by differentiation in thermal preference

482   (Larsson 2005) and that adaptive differences in thermal physiology promote ecological

483   divergence between closely related intertidal fishes (Hilton et al. 2008). However, the general

484   importance of environmental gradients for small-scale patterns of species distributions and

485   their diversification has long been a matter of debate. The traditional understanding is that

486   gradual evolution of a quantitative trait of a single population along an environmental

487   gradient would necessarily result in local adaptation to an optimum, with some smooth and

488   continuous variation around this optimum occurring due to the homogenizing effects of gene

489   flow and stabilizing selection (e.g., Kirkpatrick and Barton 1997). More recent theoretical

490   models, however, show that frequency-dependent selection due to local competition in trait

21

491   space and physical space naturally results in discrete clustering of an adaptive trait along a

492   continuous environmental gradient: these models demonstrate the plausibility of evolutionary

493   branching under such ecological conditions in asexual populations (Mizera and Meszéna

494   2003; Leimar et al. 2008), as well as the evolution of reproductive isolation in sexual

495   populations (e.g., Doebeli and Dieckmann 2003; Heinz et al. 2009). Interestingly, empirical

496   evidence for the maintenance and emergence of adaptive divergence along environmental

497   gradients is accumulating, in particular relating to depth gradients of aquatic environments

498   (Vonlanthen et al. 2009; Ingram 2011). The results presented here support the theory of

499   ecologically based adaptive diversifications along environmental gradients. The two

500   populations segregate in space, even though the underlying spatial range is continuous and

501   does not feature any intrinsic bimodality of environmental conditions.

502   There is ongoing debate among evolutionary ecologists whether or not adaptive,

503   sympatric speciation is a plausible and common scenario for the evolution of biological

504   diversity (e.g., Bolnick and Fitzpatrick 2007, Räsänen and Hendry 2008). Such a process

505   requires the evolution of two ecologically distinct and stably coexisting populations from a

506   common ancestor, as well as the emergence of reproductive isolation between the diverging

507   populations. The purpose of the present model was to identify potential ecological drivers and

508   physiological determinants of the diversifying process in a well-studied natural system. Our

509   results suggest that adaptive diversification would likely be promoted by natural selection

510   under the specific ecological conditions studied through our model. We found that

511   evolutionary diversification in the sexual model is likely if the probability of choosing the

512   same phenotype over a phenotype that differs in trait value by 1°C is greater than 65%

513   (corresponding to $\sigma_a = 0.9$). To our knowledge, no empirical estimates exist of mating

514   probabilities based on traits related to thermal preference/performance of fishes within a

515   similar ecological context. Yet, some degree of phenotype matching seems likely for the

22

516   coregonids, considering that changes in temperature preference are associated with changes in

517   habitat use, and potentially, in growth efficiency (Mehner et al. 2011). We also found that

518   diversification in the sexual model is likely if the probability that the offspring trait value

519   differs by less than 1°C from the mid-parental trait value is greater than 90% (corresponding

520   to $\sigma_{sr} = 0.6$). The resulting standing variation in a hypothetical monomorphic population

521   corresponds to a genetic coefficient of variation of 13% (Houle 1992). For comparison, a

522   value of 6% was used for the initial genetic coefficient of variation in an evolutionary model

523   parameterized for Atlantic cod (*Gadus morhua*), a value that was considered conservative

524   (i.e. low) in light of the available empirical evidence (Enberg et al. 2009).

525   Reproductive isolation between the Lake Stechlin coregonids is attained via a

526   phenological separation in terms of spawning times, with *C. albula* spawning in late autumn

527   and *C. fontanae* in spring (Schulz and Freyhof 2003). This temporal separation of

528   reproduction, which hinders gene flow between the populations, might have evolved as a by-

529   product of thermal specialization, owing to slower maturation and later spawning at lower

530   temperatures. In fact, the majority of other European populations of the *C. albula* complex are

531   autumn-spawners (Kottelat and Freyhof 2007; Mehner et al. 2010a) and generally show

532   thermal preferences far above that of *C. fontanae* in Lake Stechlin (Ohlberger et al. 2008c).

533   Another potential by-product of such a thermal adaptation is differentiation in body size, as

534   observed for the coregonids in Lake Stechlin. Mature females of *C. fontanae* are smaller (87-

535   126 mm) than those of sympatric *C. albula* (134-167 mm), with both maturing at about 1½

536   years (Schulz and Freyhof 2003). Colder water temperatures slow down the rate of energy

537   assimilation and hence of growth and maturation (Mehner et al. 2011). In consequence, cold-

538   adapted phenotypes are more likely to mature later than warm-adapted ones, which may lead

539   to a phenological separation in spawning time. This assortment may be reinforced by the lack

540   of food during winter months, which can impede maturation and thus lead to a further delay

541   in maturation until spring. Such a bimodal spawning opportunity would strengthen assortment

542   based on similarity in optimum temperature. Reproductive isolation through assortative

543   mating based on differences in spawning time and/or location, possibly in combination with

544   differentiation in body size, has been described for many species, including freshwater fishes

545   in postglacial lakes (Jonsson and Jonsson 2001; Østbye et al. 2004). It should also be noted,

546   however, that whether assortative mating preceded or followed ecological divergence remains

547   uncertain in most cases (Snowberg and Bolnick 2008).

548   While other mechanisms in principle might have brought about the temporal separation

549   in spawning times, there are no data supporting this view. Furthermore, the evolution of

550   reproductive isolation is not sufficient for explaining the stable coexistence of species if these

551   are ecologically identical (Coyne and Orr 2004). Because the two Lake Stechlin coregonids

552   have surprisingly similar diets, their differential use of thermal microhabitats appears to be

553   the only mechanism by which they have achieved ecological segregation. Whether divergence

554   in thermal-microhabitat use and the corresponding adaptations caused a shift in spawning

555   time or whether causation has worked in the opposite direction cannot be answered based on

556   present knowledge. It should also be acknowledged that the ecological conditions in the lake

557   have not been stable since the last glaciation and that past climate events might have

558   facilitated the segregation.

559   Our study highlights the potential role of temperature gradients for shaping processes

560   of ecological and evolutionary diversification through thermal adaptation. This perspective on

561   the ecologically based evolution of sympatric species is currently receiving increasing

562   scientific interest and presents a promising path for future research (Keller and Seehausen

563   2012; Svensson 2012). Prospective work may use the present model as a starting point, for

564   example, to develop a predictive evolutionary framework for evaluating the impact of future

565   temperature changes due to global warming on fish populations similar to those studied here.

566   Such an approach could provide insights into the potential implications of thermal

567   specialization for species interactions and for their adaptive responses to altered

568   environmental conditions.

569   **ACKNOWLEDGMENTS**

585 **REFERENCES**

586 Bolnick, D. I. 2004. Can intraspecific competition drive disruptive selection? An

587   experimental test in natural populations of sticklebacks. Evolution 58:608-618.

588 Bolnick, D. I., and B. M. Fitzpatrick. 2007. Sympatric speciation: models and empirical

589   evidence. Annual Review of Ecology, Evolution, and Systematics 38:459-487.

590 Bolnick, D. I., and O. L. Lau. 2008. Predictable patterns of disruptive selection in stickleback

591   in postglacial lakes. American Naturalist 172:1-11.

592 Bulmer, M. G. 1980. The mathematical theory of quantitative genetics. Clarendon Press,

593   Oxford.

594 Coyne, J. A., and H. A. Orr. 2004. Speciation. Sinauer Associates, Sunderland, MA.

595 Dieckmann, U., and R. Law. 1996. The dynamical theory of coevolution: A derivation from

596   stochastic ecological processes. Journal of Mathematical Biology 34:579-612.

597 Dieckmann, U., and M. Doebeli. 1999. On the origin of species by sympatric speciation.

598   Nature 400:354-357.

599 Dieckmann U., J. A. J. Metz, M. Doebeli, and D. Tautz. 2004. Adaptive speciation.

600   Cambridge University Press, Cambridge, MA.

601 Diekmann, O. 2004. A beginner's guide to adaptive dynamics. Pages 47-86 *in* R. Rudnicki,

602   editor. Mathematical Modelling of Population Dynamics. Volume 63 of Banach Center

603   Publications, Polish Academy of Sciences, Warszawa.

604 Doebeli, M., and U. Dieckmann. 2003. Speciation along environmental gradients. Nature

605   421:259-264.

606 Doebeli, M., and U. Dieckmann. 2005. Adaptive dynamics as a mathematical tool for

607   studying the ecology of speciation processes. Journal of Evolutionary Biology 18:1194-

608   1200.

609   Enberg, K., C. Jørgensen, E. S. Dunlop, M. Heino, and U. Dieckmann. 2009. Implications of

610   fisheries-induced evolution for stock rebuilding and recovery. Evolutionary

611   Applications 2:394-414.

612   Gavrilets, S., and A. Vose. 2007. Case studies and mathematical models of ecological

613   speciation. 2. Palms on an oceanic island. Molecular Ecology 16:2910-2921.

614   Gavrilets, S. 2005. 'Adaptive speciation': It is not that simple. Evolution 53:696-699.

615   Gavrilets, S., A. Vose, M. Barluenga, W. Salzburger, and A. Meyer. 2007. Case studies and

616   mathematical models of ecological speciation. 1. Cichlids in a crater lake. Molecular

617   Ecology 16:2893-2909.

618   Geritz, S. A. H., E. Kisdi, G. Meszéna, and J. A. J. Metz. 1998. Evolutionarily singular

619   strategies and the adaptive growth and branching of the evolutionary tree. Evolutionary

620   Ecology 12:35-57.

621   Geritz, S. A. H., M. Gyllenberg, F. J. A. Jacobs, and K. Parvinen. 2002. Invasion dynamics

622   and attractor inheritance. Journal of Mathematical Biology 44:548-560.

623   Gislason, D., M. Ferguson, S. Skúlason, and S. S. Snorrason. 1999. Rapid and coupled

624   phenotypic and genetic divergence in Icelandic Arctic char (*Salvelinus alpinus*).

625   Canadian Journal of Fisheries and Aquatic Sciences 56:2229-2234.

626   Heinz, S. K., R. Mazzucco, and U. Dieckmann. 2009. Speciation and the evolution of

627   dispersal along environmental gradients. Evolutionary Ecology 23:53-70.

628   Helland, I. P., J. Freyhof, P. Kasprzak, and T. Mehner. 2007. Temperature sensitivity of

629   vertical distributions of zooplankton and planktivorous fish in a stratified lake.

630   Oecologia 151:322-330.

631   Helland, I. P., C. Harrod, J. Freyhof, and T. Mehner. 2008. Co-existence of a pair of pelagic

632   planktivorous coregonid fish. Evolutionary Ecology Research 10:373-390.

633   Helland, I. P., L. A. Vøllestad, J. Freyhof, and T. Mehner. 2009. Morphological differences

634   between two ecologically similar sympatric fishes. Journal of Fish Biology 75:2756-

635   2767.

636   Hilton, Z., Wellenreuther, M., and K. D. Clements. 2008. Physiology underpins habitat

637   partitioning in a sympatric sister-species pair of intertidal fishes. Functional Ecology

638   22:1108-1117.

639   Houle, D. 1992. Comparing evolvability and variability of quantitative traits. Genetics

640   130:195-204.

641   Hudson, A. G., P. Vonlanthen, R. Müller, and O. Seehausen. 2007. Review: The geography of

642   speciation and adaptive radiation in coregonines. Archiv für Hydrobiologie Special

643   Issues Advances in Limnology 60:111-146.

644   Ingram, T. 2011. Speciation along a depth gradient in a marine adaptive radiation.

645   Proceedings of the Royal Society B - Biological Sciences 278:613-618.

646   Ito, H. C., and U. Dieckmann. 2007. A new mechanism for recurrent adaptive radiations.

647   American Naturalist 170:E96-E111.

648   Jonsson, B., and N. Jonsson. 2001. Polymorphism and speciation in Arctic charr. Journal of

649   Fish Biology 58:605-638.

650   Keller, I., and O. Seehausen. 2012. Thermal adaptation and ecological speciation. Molecular

651   Ecology 21:782-799.

652   Kirkpatrick, M., and N. H. Barton. 1997. Evolution of a species' range. American Naturalist

653   150:1-23.

654   Knudsen, R., A. Klemetsen, P.-A. Amundsen, and B. Hermansen. 2006. Incipient speciation

655   through niche expansion: an example from the Arctic charr in a subarctic lake.

656   Proceedings of the Royal Society B - Biological Sciences 273:2291-2298.

657   Kottelat, M., and J. Freyhof. 2007. Handbook of European freshwater fishes. Kottelat, Cornol

658   and Freyhof, Berlin.

659   Larsson, S. 2005. Thermal preference of Arctic charr, *Salvelinus alpinus*, and brown trout,

660   *Salmo trutta* - implications for their niche segregation. Environmental Biology of Fishes

661   73:89-96.

662   Leimar, O., M. Doebeli, and U. Dieckmann. 2008. Evolution of phenotypic clusters through

663   competition and local adaptation along an environmental gradient. Evolution 62:807-

664   822.

665   Lu, G., and L. Bernatchez. 1999. Correlated trophic specialization and genetic divergence in

666   sympatric lake whitefish ecotypes (*Coregonus clupeaformis*): Support for the ecological

667   speciation hypothesis. Evolution 53:1491-1505.

668   Mayr, E. 1963. Animal species and evolution. Belknap Press, Cambridge, MA.

669   Mehner, T., M. Diekmann, U. Brämick, and R. Lemcke. 2005. Composition of fish

670   communities in German lakes as related to lake morphology, trophic state, shore

671   structure and human use intensity. Freshwater Biology 50:70-85.

672   Mehner, T., K. Pohlmann, C. Elkin, M. T. Monaghan, B. Nitz, and J. Freyhof. 2010a. Genetic

673   population structure of sympatric and allopatric populations of Baltic ciscoes

674   (*Coregonus albula* complex, Teleostei, Coregonidae). BMC Evolutionary Biology

675   10:85.

676   Mehner, T., S. Busch, I. P. Helland, M. Emmrich and J. Freyhof. 2010b. Temperature-related

677   nocturnal vertical segregation of coexisting coregonids. Ecology of Freshwater Fish

678   19:408-419.

679   Mehner, T., S. Schiller, G. Staaks, and J. Ohlberger. 2011. Cyclic temperatures influence

680   growth efficiency and biochemical body composition of vertically migrating fish.

681   Freshwater Biology 56:1554-1566.

682   Metz, J. A. J., R. M. Nisbet, and S. A. H. Geritz. 1992. How should we define fitness for

683   general ecological scenarios? Trends in Ecology and Evolution 7:198-202.

684   Metz, J. A. J., S. A. H. Geritz, G. Meszéna, F. J. A. Jacobs, and J. S. Van Heerwaarden. 1996.

685   Adaptive dynamics; A geometrical study of the consequences of nearly faithful

686   reproduction. Pages 183-231 *in* S. J. Van Strien and S. M. V. Lunel, editors. Stochastic

687   and spatial structures of dynamical systems. North Holland, Amsterdam.

688   Mizera, F., and G. Meszéna. 2003. Spatial niche packing, character displacement and adaptive

689   speciation along an environmental gradient. Evolutionary Ecology Research 5:363-382.

690   Nosil, P. 2012. Ecological speciation. Oxford University Press, Oxford

691   Ohlberger, J., T. Mehner, G. Staaks, and F. Hölker. 2008a. Temperature-related physiological

692   adaptations promote ecological divergence in a sympatric species pair of temperate

693   freshwater fish, *Coregonus* spp. Functional Ecology 22:501-508.

694   Ohlberger, J., T. Mehner, G. Staaks, and F. Hölker. 2008b. Is ecological segregation in a pair

695   of sympatric coregonines supported by divergent feeding efficiencies? Canadian Journal

696   of Fisheries and Aquatic Sciences 65:2105-2113.

697   Ohlberger, J., G. Staaks, T. Petzoldt, T. Mehner, and F. Hölker. 2008c. Physiological

698   specialization by thermal adaptation drives ecological divergence in a sympatric fish

699   species pair. Evolutionary Ecology Research 10:1173-1185.

700   Østbye, K., T. F. Næsje, L. Bernatchez, O. T. Sandlund, and K. Hindar. 2004. Morphological

701   divergence and origin of sympatric populations of European whitefish (*Coregonus*

702   *lavaretus* L.) in Lake Femund, Norway. Journal of Evolutionary Biology 18:683-702.

703   Orr, M. R., and T. B. Smith. 1998. Ecology and speciation. Trends in Ecology and Evolution

704   13:502-506.

705   Pörtner, H. O., L. Peck, and G. Somero. 2007. Thermal limits and adaptation in marine

706   Antarctic ectotherms: An integrative view. Philosophical Transactions of the Royal

707   Society B - Biological Sciences 362:2233-2258.

708   Pörtner, H. O., P. M. Schulte, C. M. Wood, and F. Schiemer. 2010. Niche dimensions in

709   fishes: An integrative view. Physiological and Biochemical Zoology 83:808-826.

710   Räsänen, K., and A. P. Hendry. 2008. Disentangling interactions between adaptive divergence

711   and gene flow when ecology drives diversification. Ecology Letters 11:624-636.

712   Roughgarden, J. 1979. Theory of population genetics and evolutionary ecology. Macmillan,

713   New York.

714   Schluter, D. 2000. The ecology of adaptive radiation. Oxford University Press, Oxford.

715   Schluter, D. 2003. Frequency dependent natural selection during character displacement in

716   sticklebacks. Evolution 57:1142-1150.

717   Schluter, D. 2009. Evidence for ecological speciation and its alternative. Science 323:737-

718   741.

719   Schluter, D., and J. D. McPhail. 1993. Character displacement and replicate adaptive

720   radiation. Trends in Ecology and Evolution 8:197-200.

721   Schulz, M., and J. Freyhof. 2003. *Coregonus fontanae*, a new spring-spawning cisco from

722   Lake Stechlin, northern Germany (Salmoniformes: Coregonidae). Ichthyological

723   Exploration of Freshwaters 14:209-216.

724   Schulz, M., R. Koschel, C. Reese, and T. Mehner. 2004. Pelagic trophic transfer efficiency in

725   an oligotrophic, dimictic deep lake (Lake Stechlin, Germany) and its relation to

726   fisheries yield. Limnologica 34:264-273.

727   Snowberg, L. K., and D. I. Bolnick. 2008. Assortative mating by diet in a phenotypically

728   unimodal but ecologically variable population of stickleback. American Naturalist

729   172:733-739.

730   Somero, G. N. 2002. Thermal physiology and vertical zonation of intertidal animals: Optima,

731   limits, and costs of living. Integrative and Comparative Biology 42:780- 789.

732   Somero, G. N. 2005. Linking biogeography to physiology: Evolutionary and acclimatory

733   adjustments of thermal limits. Frontiers in Zoology 2:1.

734   Svanbäck, R., and D. I. Bolnick. 2007. Intraspecific competition drives increased resource use

735   diversity within a natural population. Proceedings of the Royal Society B - Biological

736   Sciences 274:839-844.

737   Svensson, E. I. 2012. Non-ecological speciation, niche conservatism and thermal adaptation:

738   how are they connected? Organisms Diversity & Evolution 12:229-240.

739   Swanson, B. O., A. C. Gibb, J. C. Marks, and D. A. Hendrickson. 2003. Trophic

740   polymorphism and behavioral differences decrease intraspecific competition in a

741   cichlid, *Herichthys minckleyi*. Ecology 84:1441-1446.

742   Vamosi, S. M. 2003. The presence of other fish species affects speciation in threespine

743   sticklebacks. Evolutionary Ecology Research 5:717-730.

744   Van Tienderen, P. H., and G. De Jong. 1986. Sex ratio under the haystack model:

745   Polymorphism may occur. Journal of Theoretical Biology 122:69-81.

746   Via, S. 2001. Sympatric speciation in animals: the ugly duckling grows up. Trends in Ecology

747   and Evolution 16:381-390.

748   Vonlanthen, P, D. Roy, A. G. Hudson, R. Largiadèr, D. Bittner, and O. Seehausen. 2009.

749   Divergence along a steep ecological gradient in lake whitefish (*Coregonus* sp.). Journal

750   of Evolutionary Biology 22:489-514.

751   Waxman, D., and S. Gavrilets. 2005. 20 questions on adaptive dynamics. Journal of

752   Evolutionary Biology 18:1139-1154.

753

755 **Fig. 1:** Functions used as model input (continuous lines) together with the corresponding

756 empirical data (open circles). (A) Temperature as a function of depth $[\,T(x) = T_{min} + T_{diff}\,e^{-\phi x^2}\,]$.

757 (B) Zooplankton carrying capacity density as a function of depth $[\,K(x) = Z_{min} + Z_{diff}e^{-\varphi x}\,]$. (C)

758 Foraging probability as a function of depth $[\,F(x) = (T_{max} - T(x))_+ /(T_{max} - T_{min})\,]$. (D) Capture

759 success as a function of depth $[\,n(x) = e^{-\psi x}\,]$; (E) Foraging efficiency as a function of

760 temperature $[\,r(T, T_i) = r_{min} + (1 - r_{min})e^{-\upsilon(T - T_i)^2}\,]$. (F) Maintenance costs as a function of

761 temperature $[\,m(T) = \gamma m_0 B_{mean}^{\beta} e^{\omega T}\,]$. See Online appendices A and B for further details.

762 **Fig. 2:** Pairwise invasibility plot (PIP) for trait values between 4°C and 12°C. The grey areas

763 indicate at which trait-value combinations a mutant phenotype can invade a resident

764 phenotype, i.e., where the mutant's invasion fitness is positive. The evolutionarily singular

765 strategy at which the selection gradient vanishes is indicated by the small filled circle. Based

766 on this PIP, we expect that a monomorphic population continuously evolves along the main

767 diagonal until it reaches the evolutionarily singular strategy at about 8.1°C (which implies

768 that the singular strategy is convergence stable). At this branching point, the population

769 experiences a fitness minimum and selection accordingly becomes disruptive (which implies

770 that the singular strategy is locally evolutionarily unstable).

771 **Fig. 3:** Trait-evolution plot (TEP) for trait values between 4°C and 12°C. The parts of this

772 plot that lie above and below the diagonal are fully equivalent, since the numbering of the two

773 considered morphs is arbitrary. The grey areas represent trait-value combinations for which

774 the two morphs can stably coexist, i.e., for which they form a protected dimorphism. Arrows

775 indicate the direction of the selection gradient within this coexistence area. The continuous

776 and dotted lines show the evolutionary isoclines, along which the selection gradient for one

777　morph vanishes. As explained in Fig. 2, evolutionary branching can occur at the small filled

778　circle. The dashed lines show the evolutionary dynamics after branching, which converge to

779　the protected dimorphism at which the two evolutionary isoclines intersect (large filled

780　circles). Since this intersection point is located along the parts of the isoclines that correspond

781　to a fitness maximum (continuous lines), as opposed to a fitness minimum (dotted lines), the

782　resulting dimorphism is not only protected, but also locally evolutionarily stable. The two

783　thus established resident morphs have trait values of 5.0°C and 10.0°C.

784　**Fig. 4:** Comparison of model predictions and observations of the natural system. (A)

785　Evolution of trait values over time (continuous and dashed lines) in comparison with the trait

786　values observed for the natural populations (dotted lines). The monomorphic evolution (left

787　part) is represented by the PIP in Fig. 2, whereas the dimorphic evolution after branching

788　(right part) is represented by the TEP in Fig. 3. The initial optimum foraging temperature for

789　the monomorphic population (here set to 4°C) can be randomly chosen, since they do not

790　affect the evolutionary outcome of the model. The evolutionary outcome for the optimum

791　foraging temperatures of the two resulting morphs (5.0°C and 10.0°C) is in good agreement

792　with the experimentally determined temperature preferences of the Lake Stechlin coregonids.

793　These are shown as point estimates with 95% confidence intervals on the right side of the plot

794　for *C. fontanae* (dashed line) and *C. albula* (continuous line) (Ohlberger et al. 2008c). Units

795　along the horizontal axis can be considered arbitrary, as they are freely adjustable through the

796　choice of mutational parameters. (B) Depth distributions at the evolutionary endpoint

797　(continuous and dashed curved lines) for the two populations. The resultant model-predicted

798　average depths (continuous and dashed horizontal lines) are compared with the average

799　depths observed for the Lake Stechlin coregonids (dotted lines), showing very good

800　agreement (at 17 m and 24 m, respectively; Helland et al. 2007).

801   **Fig. 5**: Evolutionary outcomes of the sexual model (white: monomorphic; gray: dimorphic)

802   depending on the widths of the assortative-mating kernel (σ_a) and of the segregation-

803   recombination kernel (σ_{sr}). The number of morphs represented by the resulting trait

804   distribution for a given combination of σ_a and σ_{sr} is determined by comparing the biomass

805   density of the single phenotype representing the evolutionarily singular strategy (trait value

806   8.1°C) to the sum of the biomass densities of the two phenotypes representing the

807   evolutionary endpoint of the asexual model (trait values 5°C and 10°C).

808   **Fig. 6**: Trait-evolution plot for the sexual model, illustrating the distribution of biomass

809   density across all phenotypes (dark grey = high biomass density, light grey = low biomass

810   density). The parameters for the two kernels are $\sigma_a = 0.2$ and $\sigma_{sr} = 0.2$, and the resolution in

811   trait space was set to a value of 0.1. The sexual model yields a dimorphic outcome similar to

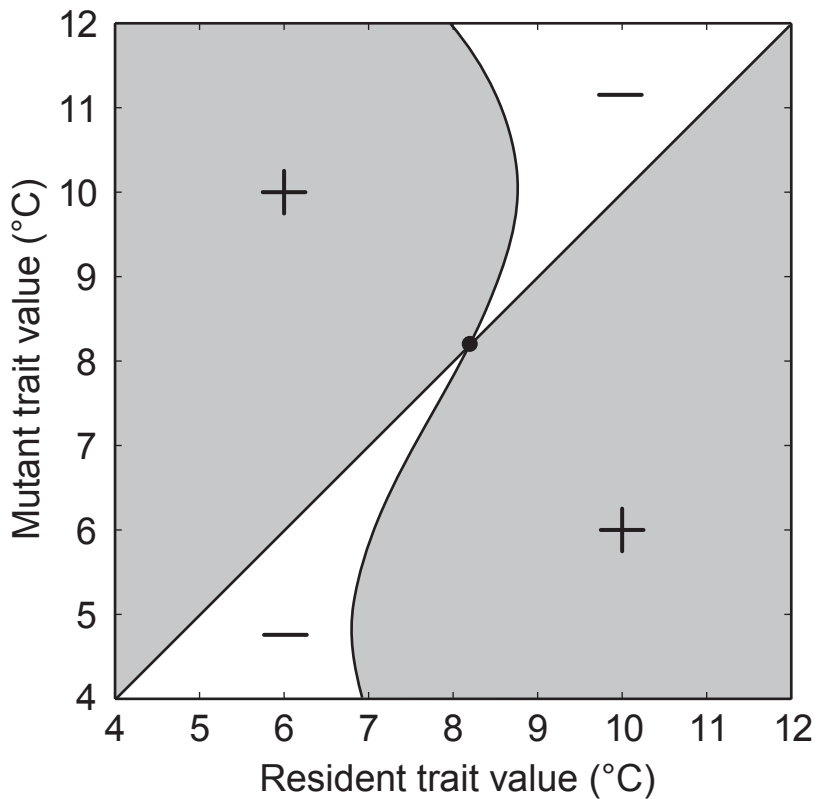812   the asexual model, with the highest biomass densities at trait values around 5°C and 10°C.

A

Trait value (°C)

Evolutionary time

B

Final density
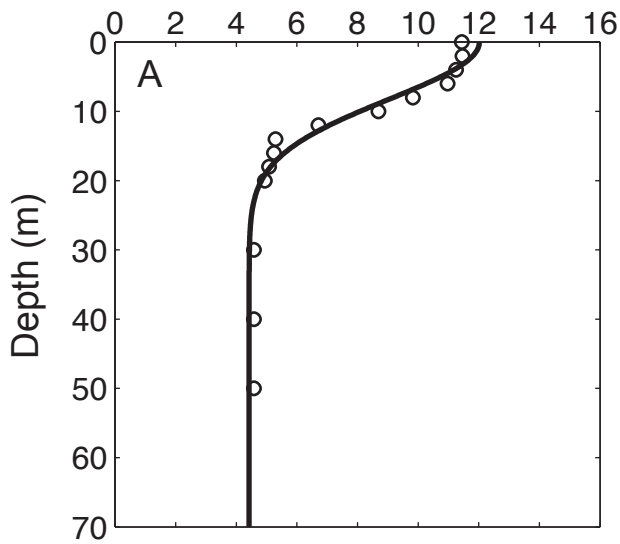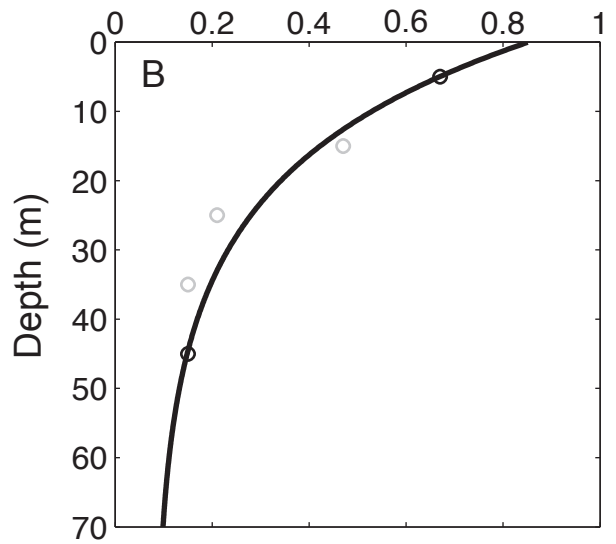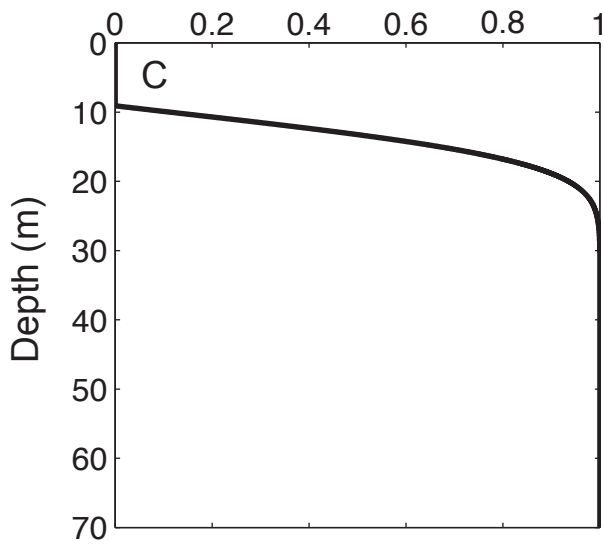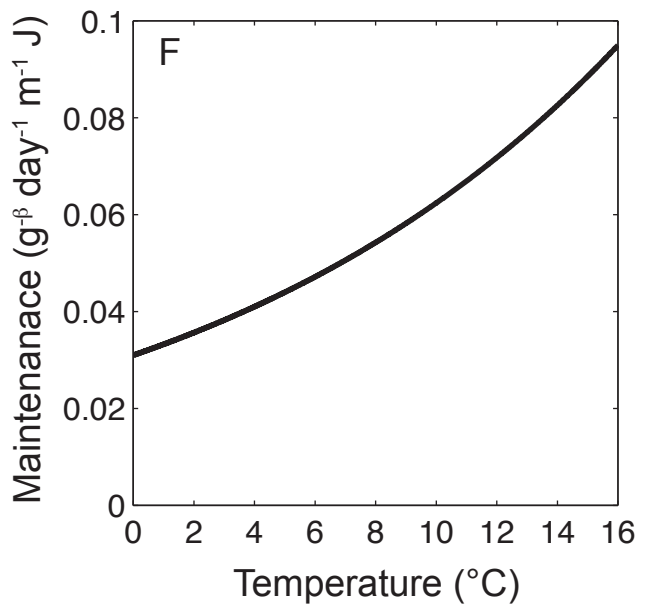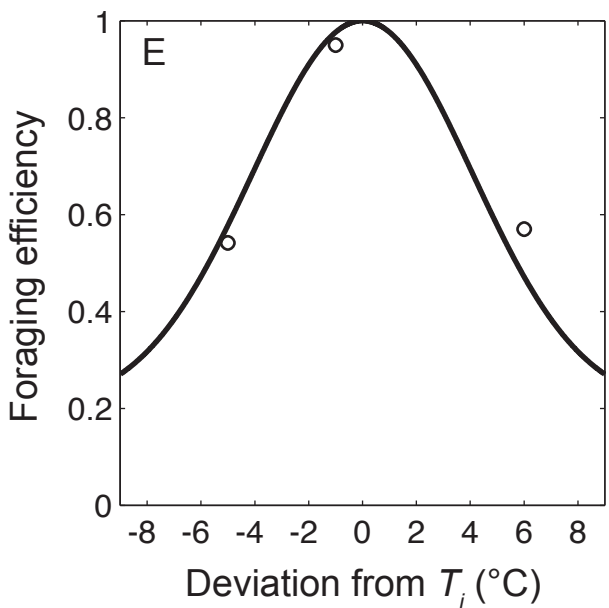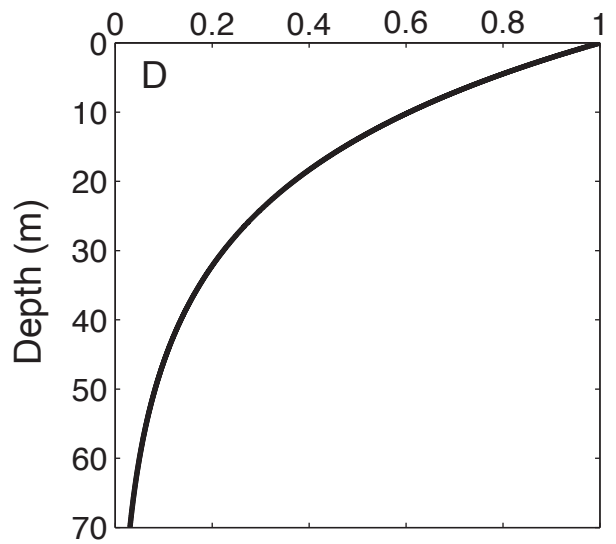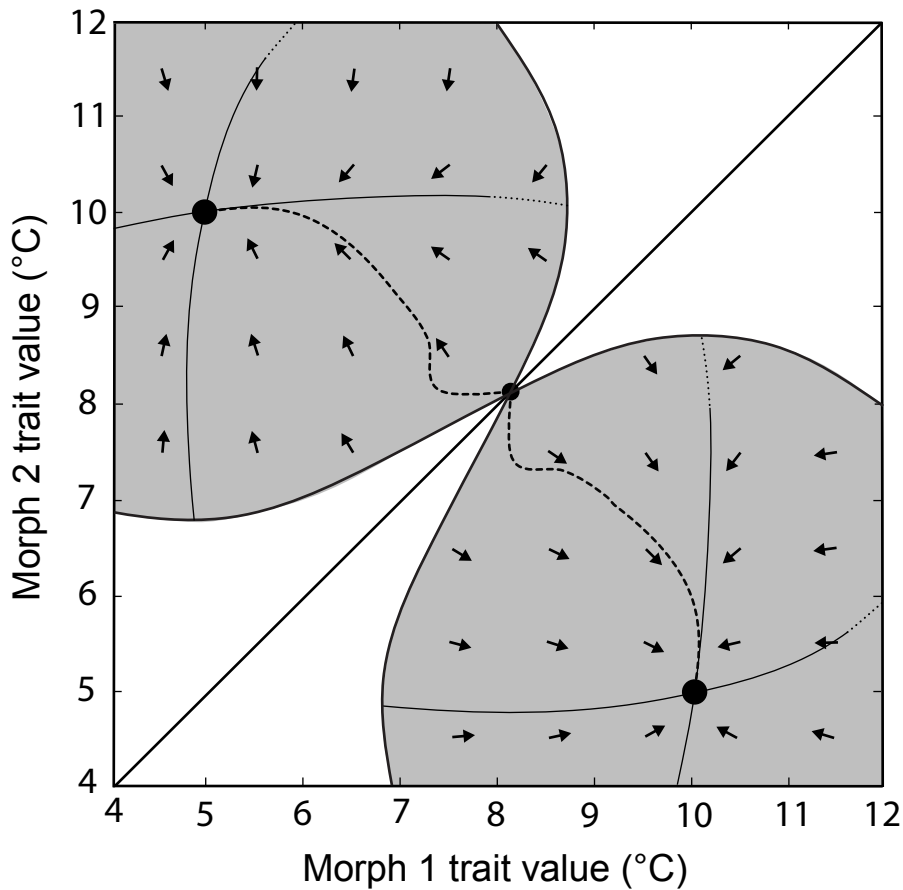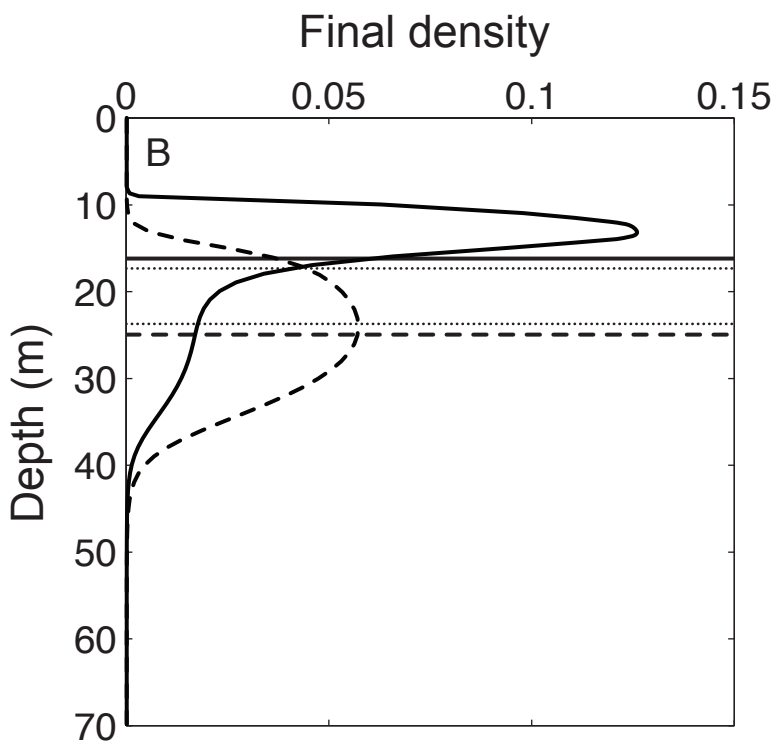
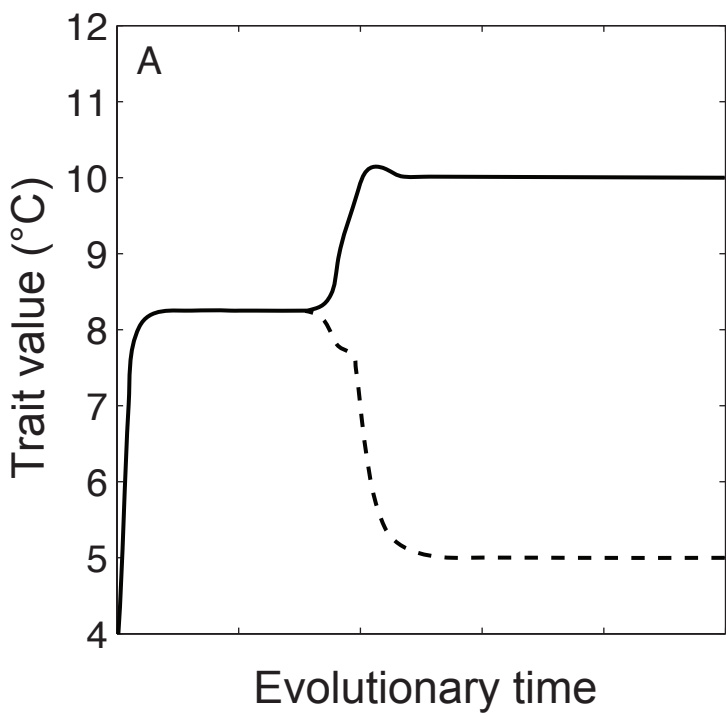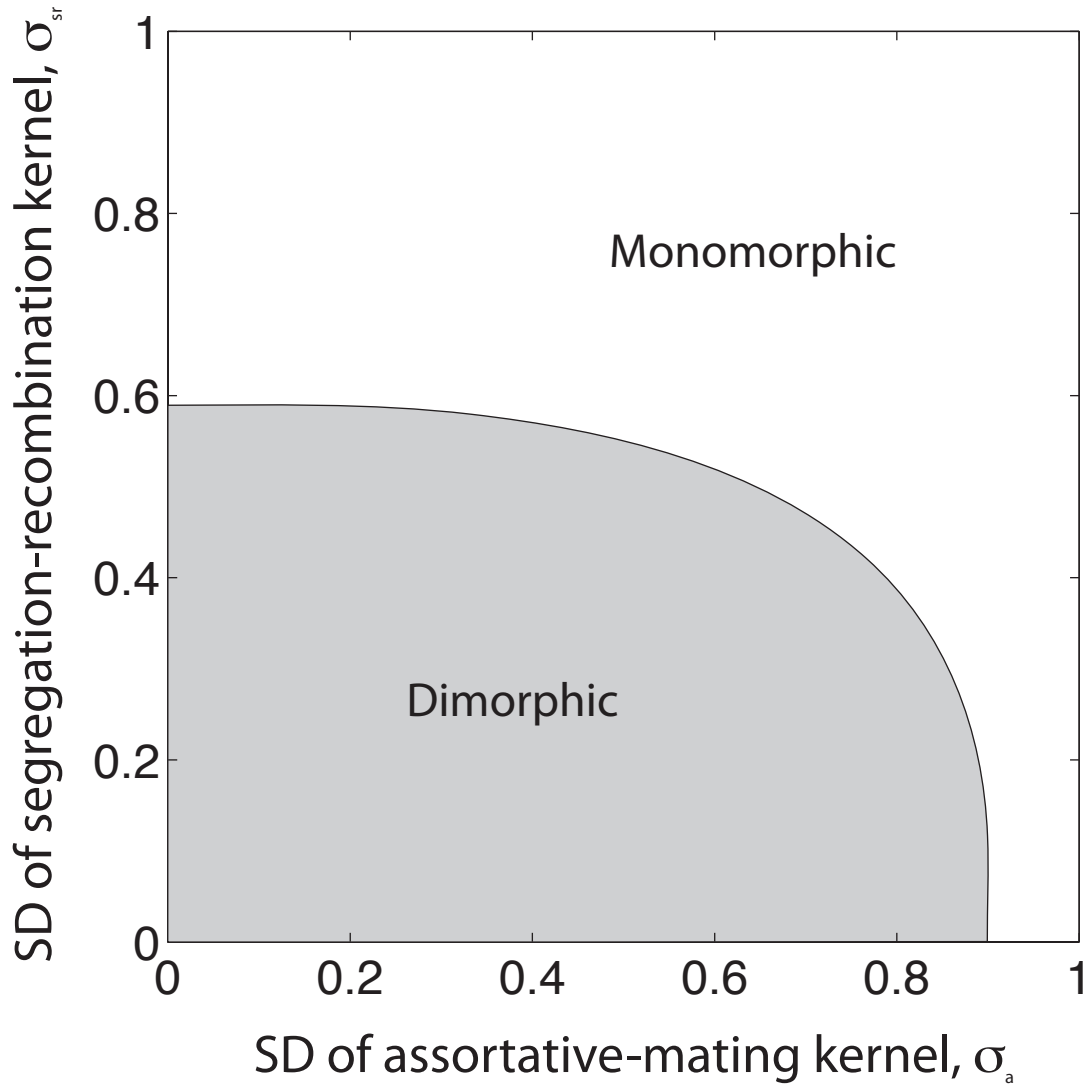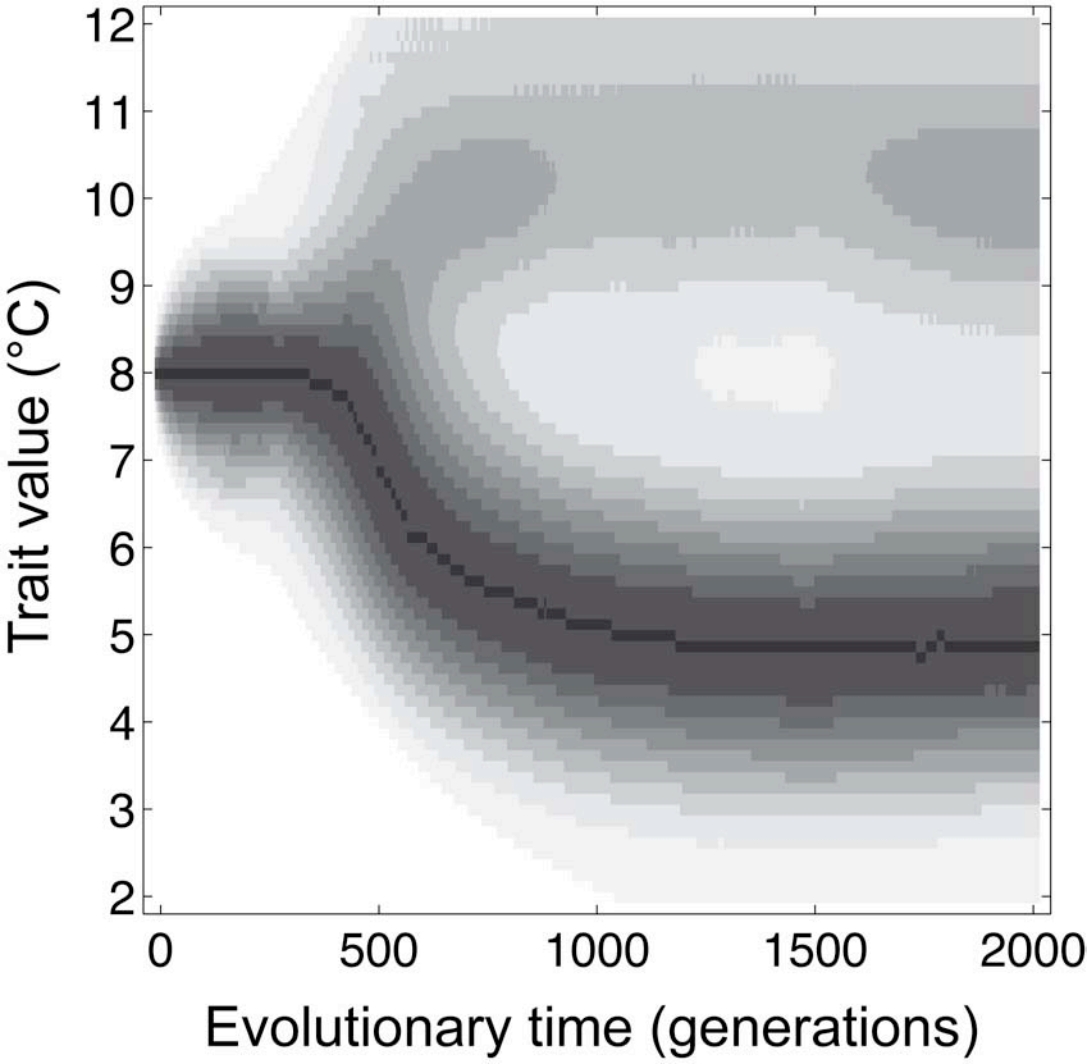Depth (m)

1   **ONLINE APPENDIX A: MODEL VARIABLES, FUNCTIONS, AND PARAMETERS**

2   **Table A1: Model variables and functions**

	Notation	Unit	Description
3			
4	x	m	Depth
5	$T(x)$*	°C	Temperature at depth x
6	T_i	°C	Temperature optimum of morph i (evolving trait value)
7	i	n.a.	Morph index ($i = 1,\dots,n$: residents; $i = 0$: rare mutant)
8	$P(x)$	g m^{-1}	Zooplankton density at depth x
9	$P_{eq}(x)$	g m^{-1}	Equilibrium zooplankton density at depth x
10	$K(x)$*	g m^{-1}	Carrying capacity of zooplankton at depth x
11	$C(x,T_i)$*	s^{-1}	Potential consumption rate of morph i with trait T_i at depth x
12	$r(T,T_i)$*	n.a.	Foraging efficiency of morph i with trait T_i at temperature T
13	$n_i(x)$*	n.a.	Capture success of morph i at depth x
14	$m(T)$*	g s^{-1} m^{-1}	Maintenance-cost density at temperature T
15	$B_i(x)$	g m^{-1}	Biomass of morph i at depth x
16	B_i	g	Total biomass of morph i
17	b_i	g	Average biomass of an individual of morph i
18	$f_i(x)$	g s^{-1} m^{-1}	Growth-rate density of morph i at depth x
19	f_i	g s^{-1}	Invasion fitness of morph i
20	g_i	g s^{-1} °C^{-1}	First derivative of invasion fitness at trait value of morph i
21	h_i	g s^{-1} °C^{-2}	Second derivative of invasion fitness at trait value of morph i

22   * Model input functions calibrated from empirical data as specified in Online appendix B

23

24 **Table A2: Model parameters**

Notation	Unit	Value (±SE)*	Source	Description
26 α	n.a.	6.0	1	Degree of foraging optimality
27 x_{max}	m	68	2	Depth of lake bottom
28 T_{min}	°C	4.42 (±0.14)	3	Minimum temperature at lake bottom
30 T_{diff}	°C	7.60 (±0.26)	3	Temperature difference between lake surface and lake bottom
32 T_{max}	°C	9.0	3	Temperature below which the fish forage
34 ϕ	m^{-2}	0.0073 (±0.0006)	3	Measure of how quickly temperature decreases with depth
36 Z_{min}	g m^{-1}	0.057	4	Minimum zooplankton density at lake bottom
38 Z_{diff}	g m^{-1}	0.78	4	Difference in zooplankton density between lake surface and lake bottom
41 φ	m^{-1}	0.047	4	Measure of how quickly the observed zooplankton density decreases with depth
44 r_{P}	day^{-1}	0.20	5	Renewal rate of zooplankton
45 r_{min}	n.a.	0.20	7	Minimum foraging efficiency

46	υ	$°C^{-2}$	0.030	7	Measure of how quickly
47					foraging efficiency decreases
48					around T_i
49	C_{max}	day^{-1}	0.040	8	Maximum consumption rate
50	ψ	m^{-1}	0.050	9	Measure of how quickly capture
51					success decreases with depth
52	λ	n.a.	0.6	10	Conversion factor from
53					zooplankton mass to fish mass
54	γ	$g\ J^{-1}$	0.00018	6	Conversion factor from energy to
55					mass
56	m_0	$g^{-\beta}\ day^{-1}\ m^{-1}\ J$	0.82 (±0.13)	7	Metabolic scaling factor
57	B_{mean}	g	10	4,7	Mean biomass of fish
58	β	n.a.	0.93 (±0.03)	7	Metabolic scaling exponent
59	ω	$°C^{-1}$	0.070 (±0.006)	7	Temperature coefficient of
60					metabolism

61 Sources: (1) Figure B1; (2) Mehner et al. 2005; (3) Mehner et al. 2010; (4) Helland et al.

62 2007, I. P. Helland, unpublished data; (5) Schulz et al. 2004; (6) Gjelland 2008; (7) Ohlberger

63 et al. 2007; (8) Binkowski and Rudstam 1994; (9) Ohlberger et al. 2008; (10) Ohlberger et al.

64 2011

65 * Standard errors could be provided for only some of the empirically estimated parameters,

66 either due to low numbers of data points or because estimates were taken from the literature

67 **REFERENCES**

68 Binkowski, F. P., and L. G. Rudstam. 1994. Maximum daily ration of Great Lakes bloater.

69   Transactions of the American Fisheries Society 123:335-343.

70   Gjelland, K. Ø. 2008. Ecological interactions, light responses and vertical habitat use in a

71   subarctic pelagic freshwater community. PhD thesis. University of Tromsø, Norway.

72   Helland, I. P., J. Freyhof, P. Kasprzak, and T. Mehner. 2007. Temperature sensitivity of

73   vertical distributions of zooplankton and planktivorous fish in a stratified lake.

74   Oecologia 151:322-330.

75   Mehner, T., F. Hölker, and P. Kasprzak. 2005. Spatial and temporal heterogeneity of trophic

76   variables in a deep lake as reflected by repeated singular samplings. Oikos 108:401-409.

77   Ohlberger, J., G. Staaks, and F. Hölker. 2007. Effects of temperature, swimming speed and

78   body mass on standard and active metabolic rate in vendace (*Coregonus albula*).

79   Journal of Comparative Physiology B 177:905-916.

80   Ohlberger, J., T. Mehner, G. Staaks, and F. Hölker. 2008. Is ecological segregation in a pair

81   of sympatric coregonines supported by divergent feeding efficiencies? Canadian Journal

82   of Fisheries and Aquatic Sciences 65:2105-2113.

83   Ohlberger, J., E. Edeline, L. A. Vøllestad, N. C. Stenseth, and D. Claessen. 2011.

84   Temperature-driven regime shifts in the dynamics of size-structured populations.

85   American Naturalist 177:211-223.

86   Mehner, T., S. Busch, I. P. Helland, M. Emmrich, and J. Freyhof. 2010. Temperature-related

87   nocturnal vertical segregation of coexisting coregonids. Ecology of Freshwater Fish

88   19:408-419.

1   **ONLINE APPENDIX B: MODEL FUNCTIONS AND THEIR ESTIMATION FROM**

2   **EMPIRICAL DATA**

3   **Temperature-depth gradient**

4   The temperature-depth gradient $T(x)$ (Fig. 1A) was estimated based on data on average year-

5   round depth-dependent temperatures in Lake Stechlin (Mehner et al. 2010). The function

6    $$T(x) = T_{min} + T_{diff}\, e^{-\phi x^2}$$

7   was fit to the data through least-square optimization. The parameters T_{min} and T_{diff} describe,

8   respectively, the minimum temperature (which is asymptotically attained at the lake bottom,

9    $x = x_{max}$) and the temperature difference between lake surface and lake bottom. The

10   parameter ϕ measures how quickly temperature decreases with depth. Lake Stechlin is a

11   stratified lake that freezes irregularly. During periods of ice cover, the stratification pattern

12   reverses. Since ice cover on average lasts only about one month (Kirillin et al. 2012), we used

13   weekly water-temperature records throughout the year to calculate average temperature as a

14   function of depth.

15   **Carrying-capacity density of zooplankton**

16   The carrying-capacity density $K(x)$ of zooplankton was estimated based on the observed

17   average zooplankton densities in the shallowest and deepest parts of Lake Stechlin, where

18   predation by the coregonids can reasonably be assumed to be negligible. The function

19    $$K(x) = Z_{min} + Z_{diff}\, e^{-\varphi x}$$

20   was fitted to the data (Helland et al. 2007; I. P. Helland, unpublished data) through least-

21   square optimization (Fig. 1B). The parameters Z_{min} and Z_{diff}, respectively, describe the

22   minimum zooplankton density (which is asymptotically attained at the lake bottom, $x = x_{max}$)

23   and the difference in zooplankton density between lake surface and lake bottom, while the

24   parameter φ measures how quickly zooplankton density decreases with depth.

25 **Dynamics of zooplankton density**

26 Changes in the depth-dependent zooplankton density $P(x)$ are determined by logistic growth

27 and Lotka-Volterra consumption,

28
$$\varepsilon \frac{dP(x)}{dt} = r_{\mathrm{P}} P(x)[1 - P(x)/K(x)] - P(x) \sum_{i=1}^{n} C(x, T_i) B_i(x),$$

29 where $K(x)$ is the carrying-capacity density of zooplankton at depth x, r_{P} is the renewal rate

30 of zooplankton, and ε is a parameter separating the timescales of zooplankton dynamics and

31 fish population dynamics. The last term in the equation above is the total zooplankton-

32 consumption density at depth x, calculated as the sum of the zooplankton-consumption

33 densities of all morphs at depth x.

34 **Equilibrium zooplankton density**

35 The zooplankton dynamics in the lake are assumed to be much faster than the fish population

36 dynamics ($\varepsilon \to 0+$). This leads to a depth-dependent equilibrium zooplankton density,

37
$$P_{\mathrm{eq}}(x) = \left(K(x) - \tfrac{1}{r_{\mathrm{P}}} \sum_{i=1}^{n} C(x, T_i) B_i(x) \right)_{+},$$

38 where $(X)_{+}$ equals X for $X > 0$ and 0 for $X \le 0$. The zooplankton dynamics are thus

39 assumed to show no temporal variation due to abiotic environmental changes or behavioral

40 responses such as diel vertical migration.

41 **Potential consumption rate**

42 The potential consumption rate $C(x, T_i)$ of a fish at depth x with trait T_i is calculated

43 according to

44
$$C(x, T_i) = C_{\max} r(T(x), T_i) n(x),$$

45 where $C_{\max}$ is the maximum consumption rate of an individual fish under optimal light and

46 temperature conditions, $r(T, T_i)$ is the foraging efficiency of a fish with trait T_i as a function

47 of temperature T, and $n(x)$ is the capture success as a function of depth x.

48   **Foraging efficiency**

49   The temperature-dependent foraging efficiency (Fig. 1E) was estimated based on empirical

50   data on the temperature-dependent swimming performance in the Lake Stechlin coregonids.

51   Specifically, it was fitted to the temperature-dependent costs of transport in $C.\ albula$, that is,

52   the energy expenditure per unit distance during swimming (Ohlberger et al. 2007), with the

53   assumption that the feeding rate of the fish scales proportionally with the distance covered

54   when foraging. It was further assumed that foraging efficiency drops symmetrically around

55   the temperature at which foraging efficiency is optimal (Ohlberger et al. 2008a),

56    $$r(T,T_i) = r_{min} + (1 - r_{min})e^{-\upsilon(T-T_i)^2}.$$

57   The same functional relationship between foraging efficiency and temperature was used for

58    $C.\ fontanae$.

59   **Capture success**

60   The depth-dependent capture success (Fig. 1D) was estimated based on measurements of the

61   feeding efficiency of the Lake Stechlin coregonids at different light levels (Ohlberger et al.

62   2008b). According to these data, the decrease in capture success with decreasing light

63   intensity was well represented by an exponential relationship,

64    $$n(x) = e^{-\psi x}.$$

65   **Maintenance costs**

66   The maintenance costs (Fig. 1F) are described as a function of temperature and biomass

67   according to the energetic models by Ohlberger et al. (2007),

68    $$m(T) = \gamma m_0 B_{mean}^{\beta} e^{\omega T},$$

69   where γ converts energy to fish mass, m_0 is the metabolic scaling factor, B_{mean} is the mean

70   biomass of a coregonid, β is the metabolic scaling exponent, and ω is the temperature

71   coefficient of metabolism.

Foraging probability

The depth-dependent foraging probability (Fig. 1C) was estimated based on observations in

Lake Stechlin showing that the coregonids rarely forage in the epilimnion at temperatures

above 9°C, although food availability is highest near the surface (Helland et al. 2007; Mehner

et al. 2010). This might be explained by the higher predation risk from perch (*Perca*

fluviatilis) in the epilimnion (Mehner et al. 2007), a species that is known to become almost

inactive at temperatures below about 9-10°C (Karås and Thoresson 1992). Foraging animals

commonly alter their behavior according to the spatial structure of prey availability and

predation risk as a consequence of a behavioral trade-off between maximizing food and

safety, also referred to as the 'landscape of fear' (Brown and Kotler 2004; Searle et al. 2008).

Consequently, we assumed that the foraging probability decreases from 1 in the coldest zones

at the lake bottom to 0 at $T_{max} = 9°C$,

$$F(x) = (T_{max} - T(x))_+ / (T_{max} - T_{min}),$$

where $(X)_+$ again equals X for $X > 0$ and 0 for $X \le 0$.

Invasion fitness of a rare mutant

Since any mutant invading a system with n resident morphs is at first very rare, the

population of mutants initially has a negligible biomass relative to the resident population.

Hence, the depth-dependent growth rate of a mutant morph can be calculated based on the

biomasses and consumption rates of the residents at equilibrium,

$$f_0(x) = C(x, T_0) P_{eq}(x) - m(T(x)).$$

The invasion fitness of the mutant is then given by

$$f_0 = \frac{1}{B_0} \int_0^{x_{max}} f_0(x) B_0(x) dx,$$

where $B_0(x)$ is the mutant population's density at depth x and B_0 is its total biomass. In

turn, $B_0(x) / B_0$ depends on the mutant's potential consumption rate, its foraging probability,

4

96 and the equilibrium resource distribution (which, as the mutant is rare, depends only on the

97 biomass distribution of the resident morphs),

98
$$\frac{1}{B_0} B_0(x) = B_i \frac{[C(x,T_0)P_{eq}(x)F(x)]^\alpha}{\int_0^{x_{max}} [C(x',T_0)P_{eq}(x')F(x')]^\alpha \, dx'} .$$

99
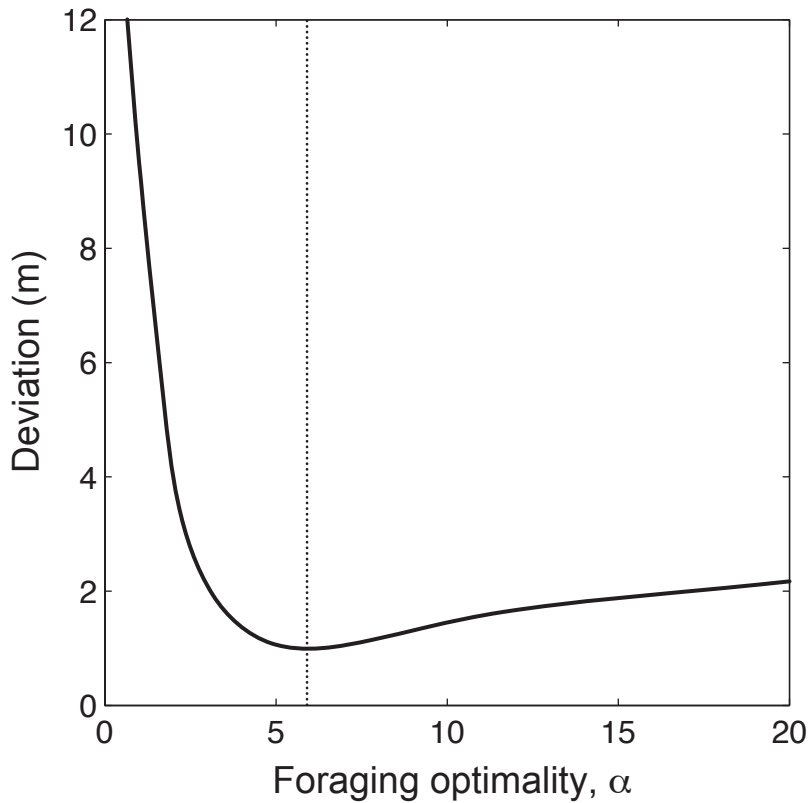
100

101 **Fig. B1:** Estimation of foraging optimality α. The foraging optimality is a measure of the

102 degree to which individuals of a population forage according to their physiological optimum,

103 the potential consumption rate, and the predation risk. The figure shows, as a function of α,

104 the sum of absolute values of the deviations between the two model-predicted and the two

105 observed average population depths of the coregonids. The least deviation occurs for a

106 foraging optimality of $\alpha = 6$, as indicated by the dotted vertical line.

107   **REFERENCES**

108   Brown J. S., and B. P. Kotler. 2004. Hazardous duty pay and the foraging cost of predation.

109   Ecology Letters 7:999-1014.

110   Helland, I. P., J. Freyhof, P. Kasprzak, and T. Mehner. 2007. Temperature sensitivity of

111   vertical distributions of zooplankton and planktivorous fish in a stratified lake.

112   Oecologia 151:322-330.

113   Karås, P., and G. Thoresson. 1992. An application of a bioenergetics model to Eurasian perch

114   (*Perca fluviatilis* L.). Journal of Fish Biology 41:217-230.

115   Kirillin, G., M. Leppäranta, A. Terzhevik, N. Granin, J. Bernhardt, C. Engelhardt, T.

116   Efremova, S. Golosov, N. Palshin, P. Sherstyankin, G. Zdorovennova, and R.

117   Zdorovennov. 2012. Physics of seasonally ice-covered lakes: a review. Aquatic

118   Sciences 74:659-682.

119   Mehner, T., P. Kasprzak, and F. Hölker. 2007. Exploring ultimate hypotheses to predict diel

120   vertical migrations in coregonid fish. Canadian Journal of Fisheries and Aquatic

121   Sciences 64:874-886.

122   Mehner, T., S. Busch, I. P. Helland, M. Emmrich, and J. Freyhof. 2010. Temperature-related

123   nocturnal vertical segregation of coexisting coregonids. Ecology of Freshwater Fish

124   19:408-419.

125   Ohlberger, J., G. Staaks, and F. Hölker. 2007. Effects of temperature, swimming speed and

126   body mass on standard and active metabolic rate in vendace (*Coregonus albula*).

127   Journal of Comparative Physiology B 177:905-916.

128   Ohlberger, J., G. Staaks, T. Petzoldt, T. Mehner, and F. Hölker. 2008a. Physiological

129   specialization by thermal adaptation drives ecological divergence in a sympatric fish

130   species pair. Evolutionary Ecology Research 10:1173-1185.

131   Ohlberger, J., T. Mehner, G. Staaks, and F. Hölker. 2008b. Is ecological segregation in a pair

132   of sympatric coregonines supported by divergent feeding efficiencies? Canadian Journal

133   of Fisheries and Aquatic Sciences 65:2105-2113.

134   Searle, K. R., C. J. Stokes, and I. J. Gordon. 2008. When foraging and fear meet: Using

135   foraging hierarchies to inform assessments of landscapes of fear. Behavioral Ecology

136   19:475-482.

1 **ONLINE APPENDIX C: SENSITIVITY ANALYSIS**

2 **Table C1: Sensitivity analysis for all model parameters (±10%) listed in Table A2**

Parameter	Change	Resultant trait values (°C)*	
		Morph 1	Morph 2
All	±0%	5.0	10.0
α	+10%	5.0	10.1
	−10%	5.0	9.9
x_{max}	+10%	5.0	10.0
	−10%	5.0	10.0
T_{min}	+10%	5.4	10.0
	−10%	4.6	10.0
T_{diff}	+10%	5.0	10.0
	−10%	5.0	10.0
T_{max}	+10%	5.1	10.8
	−10%	5.0	9.1
ϕ	+10%	5.0	10.0
	−10%	5.0	10.0
Z_{min}	+10%	5.0	10.0
	−10%	5.0	10.0
Z_{diff}	+10%	5.0	10.1
	−10%	5.0	9.9
φ	+10%	5.1	10.0
	−10%	4.9	10.0
r_{P}	+10%	5.0	10.0
	−10%	5.0	10.0

k	+10%	5.0	10.0
	−10%	5.0	10.0
r_{min}	+10%	5.0	9.9
	−10%	5.0	10.1
υ	+10%	5.0	9.9
	−10%	5.0	10.1
C_{max}	+10%	4.9	10.1
	−10%	5.0	9.9
ψ	+10%	5.0	10.0
	−10%	4.9	10.0
λ	+10%	4.9	10.1
	−10%	5.0	9.9
γ	+10%	5.0	10.0
	−10%	5.0	9.9
m_0	+10%	5.0	9.9
	−10%	4.9	10.1
B_{mean}	+10%	4.9	10.0
	−10%	5.0	9.9
β	+10%	5.1	9.8
	−10%	4.9	10.1
ω	+10%	5.0	10.0
	−10%	5.0	10.0

3   * Evaluated at the evolutionary endpoint of the asexual model